AIAA JOURNAL
Vol. 32, No. 7, July 1994

Probability Density Function Approach for Compressible Turbulent Reacting Flows

A. T. Hsu,* Y.-L. P. Tsai,† and M. S. Raju†
Sverdrup Technology, Inc., Brook Park, Ohio 44142

The objective of the present work is to extend the probability density function (PDF) turbulence model to compressible reacting flows. The probability density function of the species mass fractions and enthalpy are obtained by solving a PDF evolution equation using a Monte Carlo scheme. The PDF solution procedure is coupled with a compressible finite-volume flow solver which provides the velocity and pressure fields. A modeled PDF equation for compressible flows, capable of treating flows with shock waves and suitable to the present coupling scheme, is proposed and tested. Convergence of the combined finite-volume Monte Carlo solution procedure is discussed. Two supersonic diffusion flames are studied using the proposed PDF model and the results are compared with experimental data; marked improvements over solutions without PDF are observed.

Nomenclature

D_j = diffusion coefficients
D_t = turbulent diffusion coefficient
e = specific internal energy
H = total enthalpy
h = specific enthalpy
k = turbulent kinetic energy
M = molecular mixing model
M_t = turbulent Mach number
P = probability density function
Pr = production of turbulent kinetic energy
p = pressure
p' = pressure fluctuations
q_j = heat flux
S_p = source term for the compressibility effect
u_j = velocity
u_j' = velocity fluctuations
w_i = chemical source terms
x_i = spatial coordinates
Y_i = species mass fraction
α_2, α_3 = constants
Δ = velocity divergence
ϵ = dissipation rate of turbulent kinetic energy
ρ = density
τ_{ij} = shear stress
Φ = dissipation
$\langle . \rangle$ = ensemble mean
$\langle . | . \rangle$ = conditional mean
$(),_i$ = $\partial( )/\partial x_i$
$(),_t$ = $\partial( )/\partial t$

I. Introduction

THE most attractive feature of the probability density function (PDF) method is its ability to overcome the chemistry closure problem in turbulent reacting flow computations. Much progress has been made in both PDF theory and application during the past decade.[1] However, most of the previous developments in PDF models (using a PDF evolution equation) were restricted to low-speed combustion. The objective of the present work is to extend the PDF method to high-speed compressible flows.

High-speed compressible reacting flows present some unique challenges to PDF modeling because of the existence of shocks and strong dilatation terms. In principle, a joint PDF equation of velocity, pressure, temperature, and species mass fractions could be constructed and then solved using a Monte Carlo solver without any need for the mean velocity and turbulent fields to be determined by a finite-difference scheme.[2] Unfortunately, a shock-capturing PDF pressure solver is currently unavailable, and it may be a while before such a PDF approach would yield solutions to realistic problems encountered in industry. Thus, it appears that one alternative currently available for immediate application of the PDF method to high-speed flows is a solution procedure based on the decoupling between the velocity and the scalar fields. Because shock-capturing finite-difference and finite-volume codes have reached a certain degree of maturity, it seems, at least from the standpoint of practical application, that the use of the composition PDF together with a finite-difference or finite-volume code is more beneficial.

The PDF model and the corresponding Monte Carlo solver developed in the present work is general enough to be applied with any existing finite-volume or finite-difference codes. To demonstrate the portability of the PDF solver, we have applied it in conjunction with two versions of a finite-volume code known as RPLUS[3,4]: When used with the PDF algorithm to solve for chemical reactions, the species transport equations in the finite-volume code are replaced by the composition PDF equation.

Because the flow variables, including the mean velocity, density, pressure, turbulent kinetic energy, etc., are provided by the finite-volume flow solver, we only need to solve for the species mass fractions and energy (or enthalpy, temperature, etc.) in the Monte Carlo PDF solver. For low-speed reacting flows, there are two unclosed terms in the species and temperature joint PDF equation; namely, the turbulent diffusion term and the molecular mixing term. For high-speed flows, depending on the specific formulation chosen for the energy equation, many more unclosed terms could appear.[5] The pros and cons of various formulations are discussed in the present work. The formulation best suited for the present objective is identified and used as the basis on which a modeling procedure is proposed and tested.

In incompressible flow computations, the flow equations can essentially be solved independently of the PDF equation as the momentum and energy equations are decoupled; one only needs to transfer information from the flow solver to the PDF solver, but not vice versa. In contrast, the presence of the

Presented as Paper 93-0078 at the AIAA 31st Aerospace Sciences Meeting, Reno, NV, Jan. 11-14, 1993; received Feb. 5, 1993; revision received Dec. 8, 1993; accepted for publication Dec. 23, 1993.

*Supervisor, Computational Physics Section, LeRC Group, 2001 Aerospace Parkway.

†Senior Research Engineer, LeRC Group, 2001 Aerospace Parkway.

strong pressure and density gradients makes the coupling between flow equations and the PDF equation very important for compressible flows. Because the finite-volume solution of the flowfield is smooth, the transfer of information from the flow solver to the Monte Carlo PDF solver is straightforward, but information transfer the other way around presents a challenge because of the relatively large statistical error. A way of obtaining smooth averaged solutions from a Monte Carlo PDF solver, using a relatively small number of samples that is within the capacity of today's computing facilities, becomes an important issue in the finite-volume/Monte Carlo coupling process.

An issue related to the problem of coupling just mentioned is the convergence of a Monte Carlo procedure in solving an elliptic flow problem. Applications of PDF models to elliptic flow computations are few.[6-9] When a Monte Carlo solver is used to simulate elliptic flows, both the definition and the criteria of convergence are unclear and have been little discussed. Because the statistical error in a Monte Carlo method is often much larger than the truncation error in a finite-volume or finite-difference scheme, the convergence of a combined finite-volume Monte Carlo scheme is difficult to measure. Without special treatment, the solution often appears nonconvergent.

A combined ensemble- and time-averaging procedure for the solution is used in the present work. This averaging scheme makes the measurement of the convergence of a Monte Carlo scheme possible, and provides sufficiently smooth solutions to be fed back into the finite-volume flow solver, making the coupling between Monte Carlo and finite-volume solvers feasible.

The compressible PDF model is validated using a nonreacting supersonic flow over a 10-deg ramp, where the temperature rise across the shock is computed using the modeled PDF equation and compared with the theoretical solution. Two cases of supersonic hydrogen combustion are studied using the proposed model: a two-dimensional supersonic wall jet and a supersonic axisymmetric jet.

II. Probability Density Function Formulation for Compressible Flows

For compressible flows, the energy equation can be cast in a number of different forms. Pope uses the total enthalpy formulation of the energy equation[2]:

$$\rho H_{,t} + \rho u_j H_{,j} = -p_{,t} - q_{j,j} + (\tau_{ji} u_i)_{,j} \tag{1}$$

In the preceding equation, as well as in the equations that follow, repeated indices imply summation over the range of the indices. By neglecting molecular diffusion effects and assuming steady flow, the energy equation reduces to constant total enthalpy for a given sample particle. The total enthalpy formulation provides the simplest form of the energy equation and, if the PDF for pressure and velocities are known, the formulation can be applied to compressible flows without introducing any new modeled terms.[2] However, in the present case, the velocity field is obtained from a finite-volume solver, and the PDF for the velocity field is unknown. Without the velocity PDF, one cannot back out the temperature of each sample point from a given total enthalpy.

Kollmann[5] suggested the use of specific internal energy, which leads to a formulation with $\Delta = u_{j,j}$, the velocity divergence as a random variable. To solve for Δ, a transport equation for the velocity divergence was introduced into the PDF formulation. The resulting PDF equation produces a large number of new unknown terms that need modeling. Without enough experimental or direct numerical simulation data to establish models for these new terms, it is hard to estimate the viability of this approach.

In the present study, considering the fact that the velocity PDF is not known in our solution, the use of the specific enthalpy formulation minimizes the need for devising new models. As we shall show in what follows, the specific enthalpy formulation allows us to use existing models from previous works on second-order closure models for compressible turbulence.

The energy equation in terms of enthalpy is:

$$\rho h_{,t} + \rho u_j h_{,j} = -\frac{\mathrm{D}p}{\mathrm{D}t} - q_{j,j} + \Phi \tag{2}$$

where Φ is the dissipation due to viscosity. Neglecting Φ from the energy equation, the evolution equation for the joint PDF of species mass fractions and specific enthalpy, $P(Y_1, \ldots, Y_N, h; x_i, t)$, can be written as:

$$(\rho P)_{,t} + (\rho \langle u_j \rangle P)_{,j} + (\rho w_j P)_{,Y_j} = -(\rho \langle u_j' \mid Y_i, h \rangle P)_{,j}$$
$$- (\langle \rho D_j Y_{j,ii} \mid Y_i, h \rangle P)_{,Y_j} - \left(\left\langle \frac{\mathrm{D}p}{\mathrm{D}t} \middle| Y_i, h \right\rangle P \right)_{,h} \tag{3}$$

where the right-hand-side terms represent turbulent diffusion, molecular diffusion, and the pressure effect, respectively. All of the conditional means on the right-hand side of the equation are extra unknowns that need to be modeled.

In what follows the modeling of the unknown conditional means is discussed. Because comparing with the PDF equation for low-speed flows the only new term is the conditional mean of the material derivative of pressure, we start by deriving an appropriate model for this term.

Using C to denote the conditions in the mean, the new term can be written as

$$\left\langle \frac{\mathrm{D}p}{\mathrm{D}t} \middle| C \right\rangle = \langle p \mid C \rangle_{,t} + \langle u_i p_{,i} \mid C \rangle \tag{4}$$

Decomposing the random variables into means and fluctuations, $p = \langle p \rangle + p'$ and $u_i = \langle u_i \rangle + u_i'$, we have

$$\left\langle \frac{\mathrm{D}p}{\mathrm{D}t} \middle| C \right\rangle = \langle p \rangle_{,t} + \langle u_i \rangle \langle p \rangle_{,i} + \langle u_i' p' \mid C \rangle_{,i} + \langle p' u_{i,i}' \mid C \rangle \tag{5}$$

To use existing models for the last two terms in the preceding expression, we need to first assume that the product of the fluctuating velocity and fluctuating pressure is statistically independent of the species mass fractions and specific enthalpy.

With this assumption, the last two unknown terms can be readily modeled: The first of the two terms, $\langle u_i' p' \rangle_{,i}$, is the trace of the pressure-strain rate tensor in second-order closure models. Most second-order closure models give the following expression for this term[10]:

$$\langle u_i' p' \rangle_{,i} = 0.8 \rho \langle k \rangle \langle u_i \rangle_{,i} \tag{6}$$

where $\langle k \rangle$ is the mean turbulent kinetic energy.

The last term, $\langle p' u_{i,i}' \rangle$, is the so-called pressure dilatation term in second-order closure models for compressible flows. Following Sarkar et al.,[11] we write:

$$\langle p' u_{i,i}' \rangle = -\alpha_2 \rho Pr M_t + \alpha_3 \rho \epsilon M_t^2 \tag{7}$$

where α_2 and α_3 are model constants given by Sarkar et al. as 0.15 and 0.2, respectively. All the information needed in the preceding models is available from a flowfield solution using a k-ϵ model.

In the present study, the turbulent diffusion is simulated using a simple gradient diffusion model developed by O'Brien[12] and Pope[13]:

$$-\langle u_j' \mid Y_i, h \rangle P = D_t P_{,j}$$

The use of this gradient diffusion model is consistent with the use of a k-ϵ model in the flow solver.

The molecular diffusion term is modeled using the continuous mixing model by Hsu and Chen[14] and Hsu.[15] This model is an extension of Curl's model. In the modified Curl model,[16] the change of Y_n due to molecular mixing is achieved by the

following binary interaction process: divide the flow domain into small cells, each containing N sample particles. Given a small time interval δt and a turbulent time scale τ, select randomly N_{mx} pairs of particles,

$$N_{mx} = 0.5 \frac{\delta t}{C\tau} N \tag{8}$$

($C = 6.0$) and let a pair, say, m and n, mix as follows

$$Y_n(t + \delta t) = AY_m(t) + (1 - A)Y_n(t) \tag{9}$$

$$Y_m(t + \delta t) = AY_n(t) + (1 - A)Y_m(t) \tag{10}$$

where $A = 0.5\xi$, with ξ being a random variable uniformly distributed on the interval [0, 1]. The remaining $N - 2N_{mx}$ particles remain unchanged:

$$Y_n(t + \delta t) = Y_n(t) \tag{11}$$

This model does not represent the true physical process, as the properties of the sample particles change discontinuously regardless of the size of the time interval δt. This deficiency can be best illustrated by rearranging Eq. (9) and dividing it by δt

$$\frac{[Y_n(t + \delta t) - Y_n(t)]}{\delta t} = \frac{A}{\delta t} [Y_m(t) - Y_n(t)] \tag{12}$$

The derivative dY_n/dt does not exist because as δt goes to zero the right-hand side of the equation becomes infinite because both A and the difference between $Y_m(t)$ and $Y_n(t)$ are finite. This means that there is a sudden jump in the value of the scalar quantities, which is typical of a Poisson process, but is nonphysical in the present case because the flow properties of turbulence are continuous.

One can see from the preceding section that the modified Curl model relies on the parameter N_{mx} to control the extent of mixing. On the individual particle level, it assumes complete mixing once the particle is selected to participate in the mixing process, without considering the size of δt.

To achieve continuous mixing, we propose the following model: during a time interval δt, we assume that all of the particles within a cell participate in mixing. The extent of the mixing is controlled at the individual particle level. That is to say, the N particles within a given cell are randomly grouped into $N/2$ pairs; the properties of all of the particles change according to Eqs. (9) and (10). The extent of mixing now has to be controlled at the individual particle level through the parameter A, which is redefined as

$$A = C'\xi \frac{\delta t}{\tau} \tag{13}$$

where $C' = 2.0$. With this new definition, Eq. (12) can be written, in the limit $\delta t \to 0$,

$$\frac{dY_n}{dt} = C' \frac{\xi}{\tau} [Y_m(t) - Y_n(t)] \tag{14}$$

The preceding equation states that the change of Y_n due to mixing is proportional to the difference between Y_m and Y_n, and inversely proportional to the turbulence time scale τ.

The preceding model had been extensively tested on simple flows.[14,15] In fact, numerical tests showed that for mixing in homogeneous turbulence, the model gives a PDF distribution closer to the desired Gaussian distribution than the modified Curl model, and unlike solutions from the modified Curl model, the higher moments does not grow unbounded.

The final modeled PDF equation then becomes:

$$(\rho P)_{,t} + (\rho\langle u_j\rangle P)_{,j} + (\rho w_j P)_{,Y_j} = (D_t P_{,j})_{,j} + M(P) - (S_p P)_{,h} \tag{15}$$

where the first two terms on the right-hand side of the equation are the modeled terms for turbulent diffusion and molecular mixing; the last term is the term representing the compressible effect, with a new source term defined as

$$S_p = \langle p\rangle_{,t} + \langle u_i\rangle\langle p\rangle_{,i} + 0.8\rho\langle k\rangle\langle u_i\rangle_{,i} - \alpha_2\rho PrM_t + \alpha_3\rho\epsilon M_t^2 \tag{16}$$

which can be regarded as the convection velocity of a sample particle in the h direction in the space spanned by h and the various Y_i.

III. Solution Procedure

A fractional step Monte Carlo method developed by Pope[13] is used in solving the PDF evolution equation. This method has been used extensively and is well documented. The numerical schemes used in the finite-volume code are also well documented.

When coupling a PDF solver with RPLUS, the species transport equations in the RPLUS code are no longer needed. The information we need, at each marching time step, from the flow solver (RPLUS) includes the mean velocity, pressure, density, and a turbulence time scale or quantities such as the turbulent kinetic energy and dissipation rate. The species transport and chemical reactions are simulated by solving the PDF evolution equation. At every time step, the species mass fractions from the PDF solution are fed back to the mean flow solver for the computation of temperature and pressure. The Monte Carlo and finite-volume solvers are run in parallel, and information exchange occurs at every time step until a converged solution is obtained.

For steady flow problems, a combined ensemble- and time-averaging procedure is used to overcome the convergence problem in the Monte Carlo solution procedure. A time averaging is performed over a set of ensemble-averaged solutions to obtain a smoother solution. This averaging procedure is performed continuously at every time step; for instance, supposing that we are averaging over m time steps, at the nth time step, the information from time step $n - m$ is discarded, and the ensemble-averaged solution from the current time step is added to the time averaging process. A similar time averaging method has been used by Correa and Pope.[9]

The curves in Fig. 1 shows the convergence history from averaging over 1-1000 iteration steps. The large jumps in the curves are caused by abandoning the sample from the initial condition; for instance, for the error curve of averaging over 1000 time steps, the jump occurs at $N = 1000$, where N is the number of iterations. This type of large excursion in the error only happens when $N = N_{\text{average}}$, and does not appear again at larger iterations.

In the preceding example, we have assumed the time step used in the Monte Carlo computation to be large enough that the errors in the solutions of two consecutive time steps are statistically independent. When time steps used are very small,

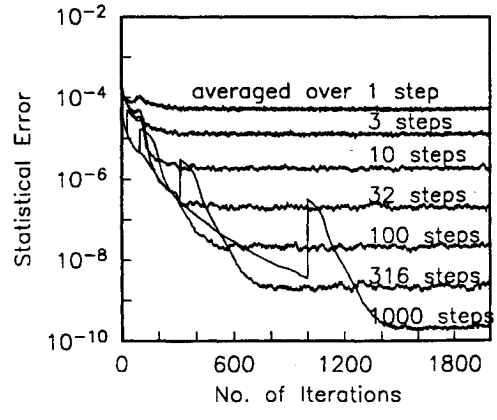

Fig. 1 Convergence history of the PDF solver measured by an L2 norm, combined time and ensemble averaged solutions.

this assumption may not be valid, and the effect of time averaging is greatly diminished. In such cases, we chose to select solutions from every M time steps for the time-averaging process, and make sure that the correlation of the random error reaches zero for a time $t > M\Delta t$. In some of the computations reported in this paper, we used solutions from every 10 time steps in the averaging process.

IV. Results and Discussion

The ability of the current PDF model to treat flows with shock waves is tested by calculating the temperature rise caused by an oblique shock. The PDF procedure is validated using experimental data for two cases of supersonic hydrogen diffusion flames: a supersonic hydrogen round jet and a supersonic wall jet. The solution procedures and numerical results are presented in the following sections.

A. Oblique Shock Calculation

The new term in the PDF equation simulates the compressibility effect; in other words, it transfers information of a compressible flowfield to the PDF solution. As a test case for the preceding model, a nonreacting supersonic flow over a 10-deg ramp is calculated using a 40×50 grid. The PDF solution of the temperature across the oblique shock is shown in Fig. 2. The PDF solutions are taken from several different times in the solution procedure. Because only 100 particles per cell were used for the calculation and no time-averaging or smoothing schemes were used, the oscillation in the solution is expected. A step function in the figure shows the theoretical solution of temperature for the same shock. The results show that the new model picks up the temperature rise across the shock fairly accurately.

A word of caution must be given here: The source term S_p can be very large for high Mach number flows or flows with strong shocks. When using an explicit time marching scheme in the Monte Carlo simulation, the time step must be carefully chosen such that the Courant-Friedrichs-Lewy number does not exceed one to ensure a converged solution.

B. Supersonic Round Jet

The numerical computations for the supersonic burner in Fig. 3 have been performed by the code that was originally developed for the modeling of turbulent reacting flows with sprays occurring inside a Wankel engine, which evolved from the RPLUS code. The finite-difference formulation is based on an Eulerian-Lagrangian approach where the unsteady, Navier-Stokes equations for a perfect gas mixture with variable properties together with the standard two-equation k-ϵ turbulence equations are solved in generalized, Eulerian coordinates on a moving grid by making use of an implicit finite-volume, Steger-Warming flux vector splitting scheme, and the liquid-phase equations are solved in Lagrangian coordinates.

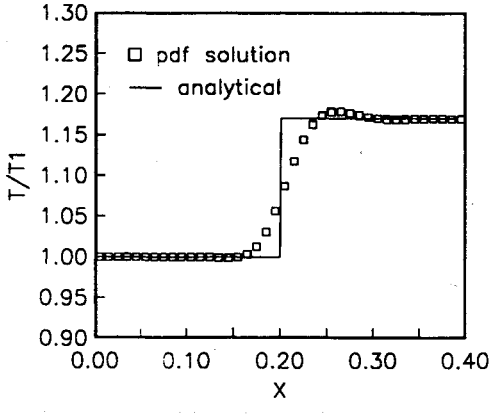

Fig. 2 Temperature rise through an oblique shock predicted by the PDF turbulence model compared with an analytical solution.

D = 0.0653 m
d = 0.009525 m
Injector lip thickness = 0.0015 m

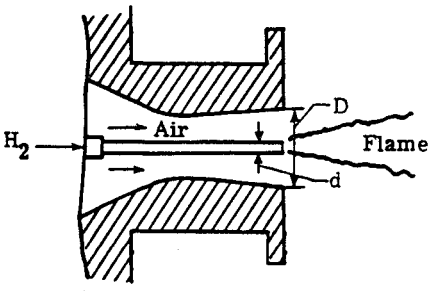

	Hydrogen jet	Free stream
Mach number, M	2.00	1.90
Temperature, T, K . . .	251	1495
Velocity, u, m/s . . .	2432	1510
Pressure, p, MPa . . .	0.1	0.1
Mass fraction:		
a_{H_2}	1.000	0
a_{O_2}	0	0.241
a_{N_2}	0	0.478
a_{H_2O}	0	0.281

Fig. 3 Geometry and test conditions for the coaxial hydrogen jet combustion.

The turbulent viscosity is computed by a compressibility correction as proposed by Villasenor et al.[17] A complete description of the code can be found in Ref. 4. The code has recently been modified to accommodate axisymmetric flowfields before being coupled with the PDF solver.

Combustion is modeled by the following global, five-species, two-step model developed by Rogers and Chinitz[18] for H_2-O_2 combustion:

$$H_2 + O_2 \overset{kf1}{\rightleftharpoons} 2OH$$

$$2OH + H_2 \overset{kf2}{\rightleftharpoons} 2H_2O$$

where the forward reaction rates are given as

$$k_{fi} = A_i T^{N_i} \exp(-E_i/RT)$$

with the coefficients given as:

$$A_1 = 11.4 \times 10^{47}, \quad N_1 = -10, \quad E_1 = 20.35 \times 10^6$$
$$A_2 = 2.5 \times 10^{64}, \quad N_2 = -13, \quad E_2 = 177.82 \times 10^6 \tag{17}$$

The unit of A_i is m^3/mole·s, and the units of E_i is J/k − mole. The backward reaction rates are calculated from the Gibbs free energy and the equilibrium coefficients.

The global model is reported to predict the oxidation of hydrogen adequately in flows that are not dominated by long ignition delay times. The model is tested for pressures at 1 atm, initial mixture temperatures of 1000–2000 K, and fuel/oxidizer equivalence ratios ranging between 0.2–2.0.

The geometry and flow conditions for the coaxial-jet case are given in Fig. 3. This flow represents mixing between two ideally expanded coaxial streams with hydrogen as the inner jet at Mach 1.9 and high-temperature vitiated air as the outer stream at Mach 2. The test conditions are taken from Evans et al.[19] This test case has been the subject of investigation by several authors,[20,21] where the flow field is modeled by differ-

ent assumptions: turbulence is modeled by making use of either algebraic or two-equation k-ϵ models, combustion is modeled by either finite-rate or equilibrium chemistry models, and/or the effect of turbulence on reaction rates is modeled by either the eddy-breakup model or the assumed probability density function approach to describe the species fluctuations.

The computational grid used in the flow calculations is 51×61 with the grid extending 30.0 fuel-injector diameters in the flow direction and 6.5 fuel-injector diameters in the transverse direction. The grid is stretched in such a way so that more resolution is obtained within 1.75 fuel-injector diameters about the centerline in the transverse direction and more resolution is also provided near the inflow in the axial direction. The flow computations are initiated at $x/d = 0.33$, the nearest point at which the measurements are made. At the inflow all of the flow variables are specified. The initial conditions used in the computations are similar to those chosen by Evans et al.,[19] except the gas composition of the central jet, which is assumed to contain small amounts of H_2O and N_2 mass fractions (=0.1) instead of pure hydrogen. The specification of inflow conditions contains a slight degree of uncertainty because the only available information at this location is the measured pitot pressures, and all of the other variables are chosen approximately to fit the measured pressure data. At the exit all of the flow variables are extrapolated from the interior. The treatment of the upper boundary is determined by applying inviscid wall conditions. Values along the centerline are obtained by applying zero gradient extrapolation, except the radial velocity, which is set equal to zero.

The PDF solution is obtained by making use of 100 particles per cell. The species mass-fraction field that is supplied to the finite-volume solver from the Monte Carlo solver is obtained from averaging the PDF solutions over the previous 100 time steps. The combined Monte Carlo and finite-volume solver required about 0.7 ms of CPU time per time step per cell on a Cray Y-MP. The inclusion of the PDF solver is found to increase the computational effort by a factor of 2.2. For the

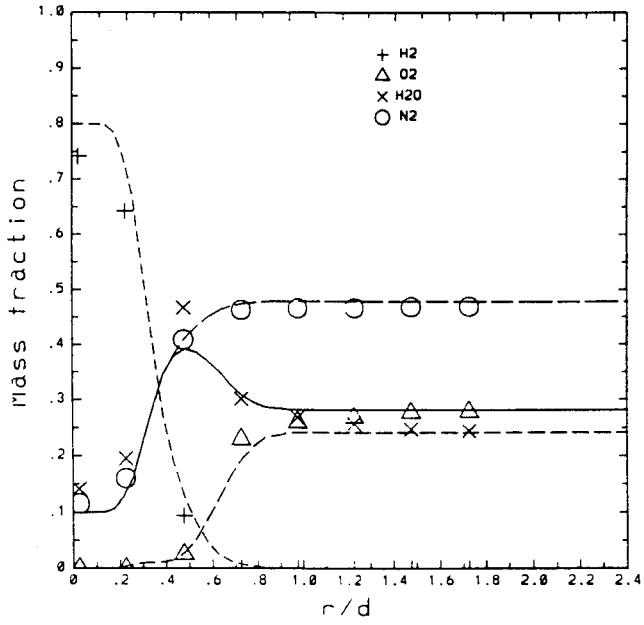

Fig. 4a Radial profiles of the predicted and measured mass fractions of major species for the PDF-CFD solver at $x/d = 8.26$.

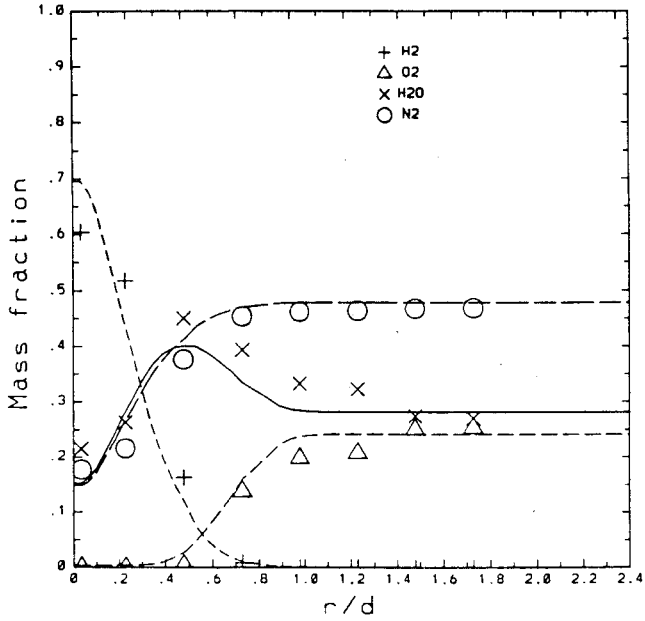

Fig. 4b Radial profiles of the predicted and measured mass fractions of major species for the PDF-CFD solver at $x/d = 15.5$.

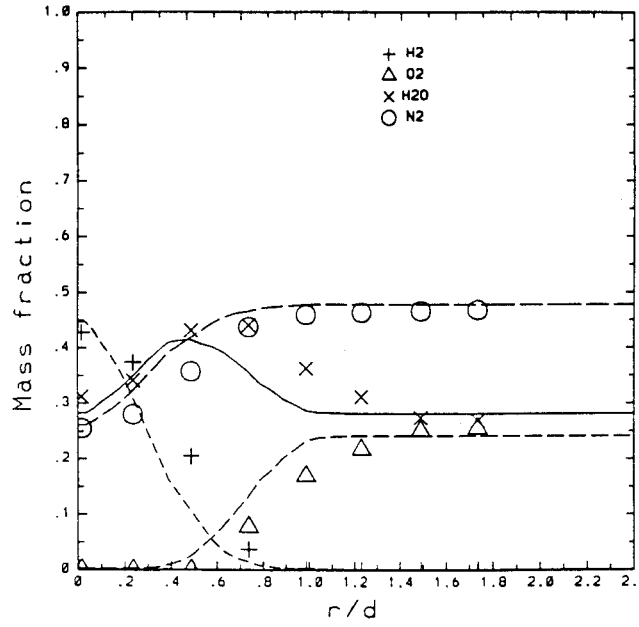

Fig. 4c Radial profiles of the predicted and measured mass fractions of major species for the PDF-CFD solver at $x/d = 21.7$.

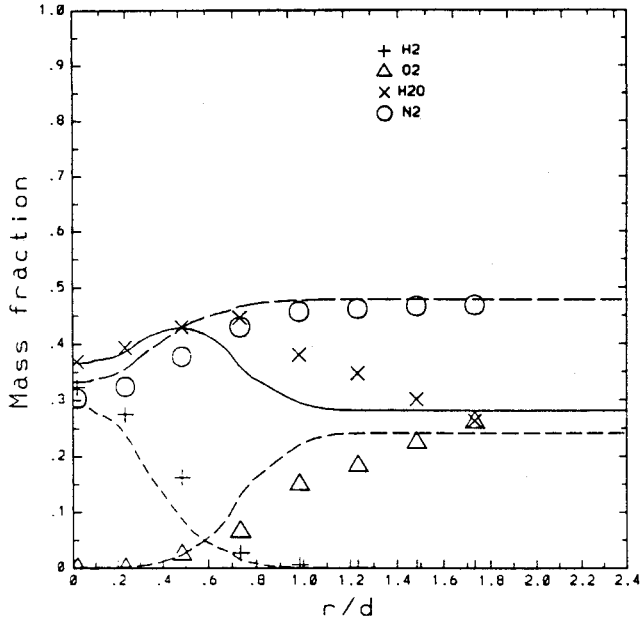

Fig. 4d Radial profiles of the predicted and measured mass fractions of major species for the PDF-CFD solver at $x/d = 27.9$.

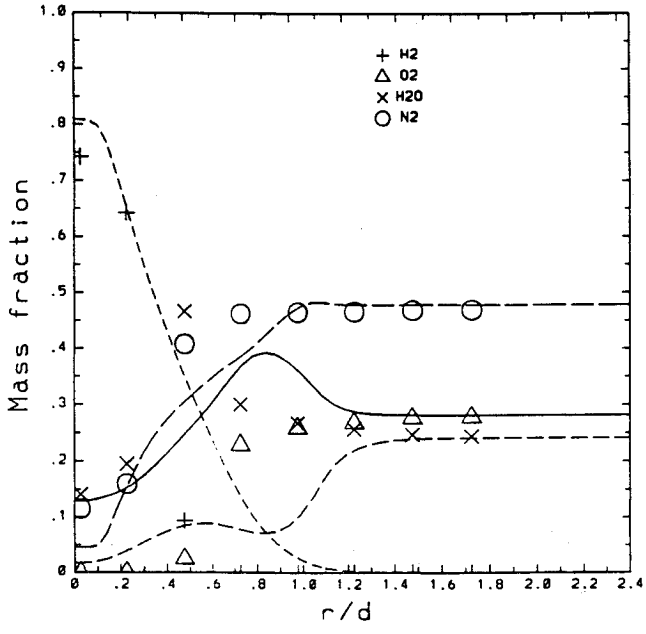

Fig. 5a Radial profiles of the predicted and measured mass fractions of major species for the CFD solver at $x/d = 8.26$.

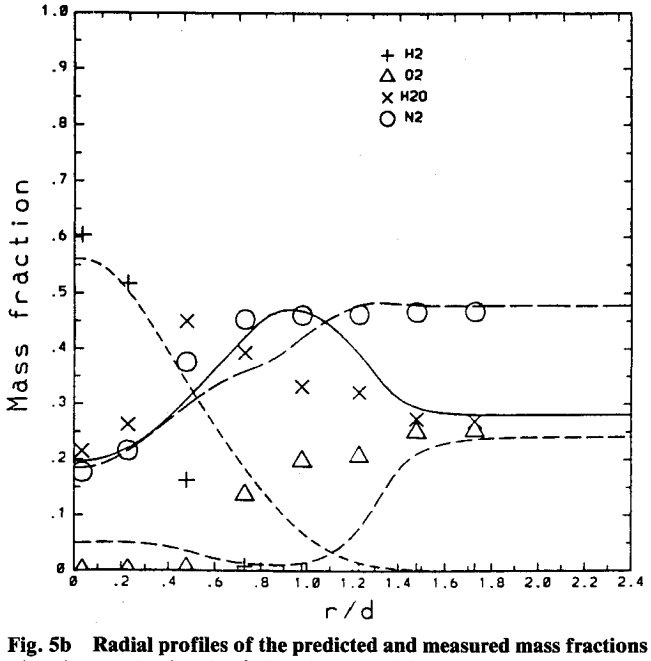

Fig. 5b Radial profiles of the predicted and measured mass fractions of major species for the CFD solver at $x/d = 15.5$.

case examined, less than 2000 time steps are required for the computations to reach a converged solution.

Figures 4a–4d show the comparisons between the PDF solutions and experimental data: radial profiles of four major species, H_2, O_2, H_2O, and N_2, are given at four different axial locations, $x/d = 8.26$, 15.5, 21.7, and 27.9, respectively. The numerical results match fairly well with the experimental data considering both the fact that the estimated error in measurements could be as large as 15%,[19] and the uncertainty involved in specifying the inflow conditions. The estimated error in the measurements is reportedly due to the possibility that the gas composition might be altered because of additional reactions taking place in the gas sampling probes as a gas chromatograph is used to measure the species concentrations.[19] The disagreement in the calculated results showing lower than the experimental values for the mass fractions of H_2O, O_2, and H_2 at axial locations of $x/d = 21.7$ and 27.9 might also be attributed to the uncertainty involved in the specification of the inflow conditions in the jet region. However, no effort is made in the present computations to study the effect of different inflow conditions on the ensuing flowfield.

To examine the effect of the PDF model on the predicted results, a separate set of finite-volume computations were performed without the PDF solver, where the chemical reaction rates are evaluated using the mean temperature and species mass fractions. The assumption of equal turbulent diffusivity is made in the computation. Combustion in these computations is also modeled by the global, two-step combustion model of Rogers and Chinitz, and the corresponding results are summarized in Figs. 5a–5d. The combined Monte Carlo and finite-volume computations seem to predict the position of the peak H_2O mass fraction rather accurately, whereas in the finite-volume computations the position of the flame zone is shifted radially outward into the high-temperature region indicating that much more O_2 is consumed than what is observed experimentally. Although Monte Carlo/

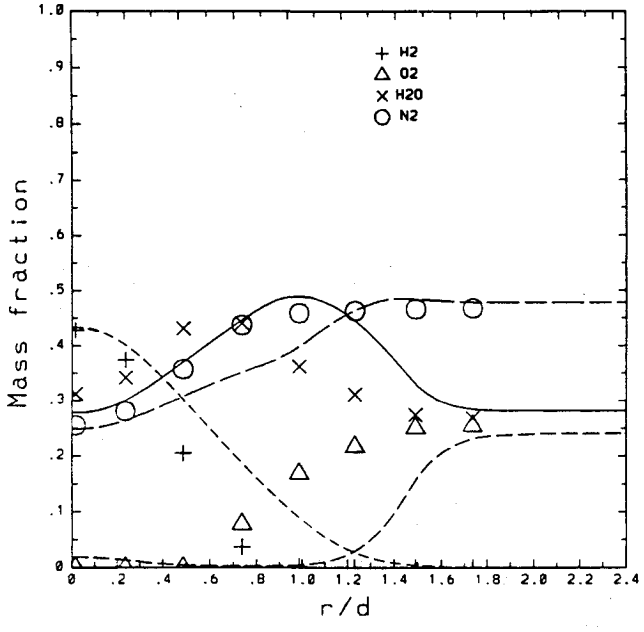

Fig. 5c Radial profiles of the predicted and measured mass fractions of major species for the CFD solver at $x/d = 21.7$.

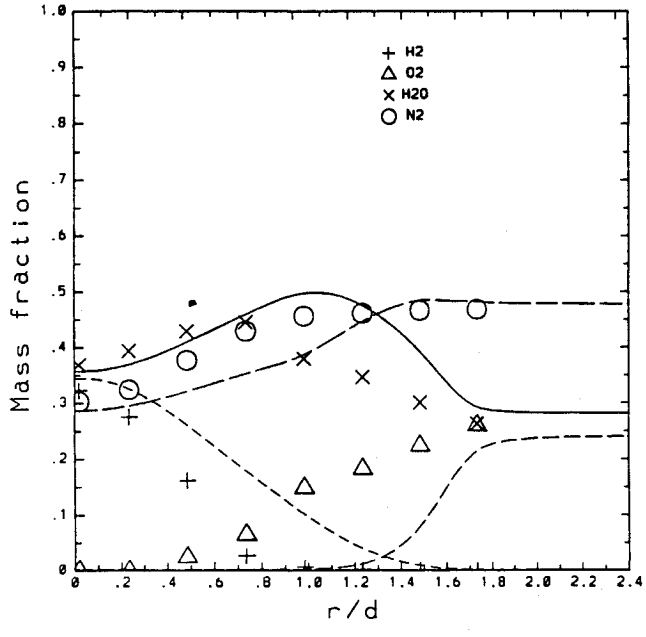

Fig. 5d Radial profiles of the predicted and measured mass fractions of major species for the CFD solver at $x/d = 27.9$.

finite-volume computations predict negligible amounts of oxygen within the central-jet region, the non-PDF computations predict substantial amounts of O_2 within this region at axial locations of $x/d = 8.26$ and 15.5. The reasons for this discrepancy could be attributed to a lack of consideration of the temperature fluctuations on the reaction rate. If the neglected temperature fluctuations are large, the reaction rates based on the mean gas temperatures are likely to lead to smaller oxidation rates as the calculated gas temperatures in this region remain lower than 600 K. At succeeding axial locations, the H_2O mass fraction grows and spreads much faster in the non-PDF solution as compared with the PDF solution. Similar to the findings in the present non-PDF computations, most, if not all of the previous computations reported a radially outward shift in the location of the peak H_2O mass fraction into the high-temperature region, and also reported that O_2 is consumed more rapidly in the calculated results. The most likely cause for this disagreement may be due to incorrect temperature dependence on some of the reaction rates, leading to rapid combustion as the temperature rises in the flame zone.[21]

The preceding results demonstrated that the use of the PDF turbulence model can improve the accuracy of combustion computations considerably.

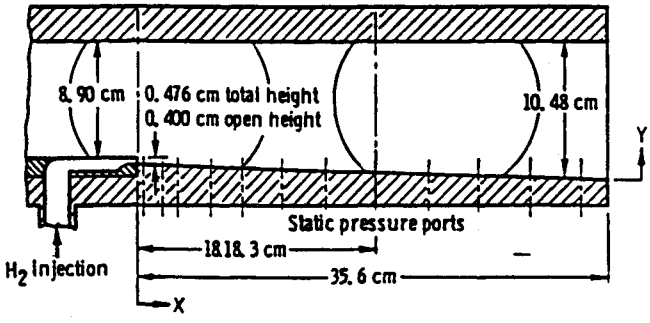

Fig. 6 Flow configuration of the experiments of Burrows and Kurkov.

C. Supersonic Wall Jet

The second test case is the experiment reported by Burrows and Kurkov[22] in 1973. This experiment has been investigated numerically by several authors: In Ref. 21, the inclusion of unmixedness did not produce the expected results for this particular case; and in Ref. 22, the numerical prediction was not very successful in part because of the assumption of equilibrium chemistry being used. Figure 6 shows its flow configuration. The two-dimensional test section measures 35.6 cm downstream of an H_2 wall jet. The mixing of the jet with a vitiated air stream supports H_2-air combustion. A high-pressure gas generator supplied Mach 2.44 vitiated air at approximately 1270 K. The composition of the air is 25.8% O_2, 25.6% H_2O, and 48.6% N_2 by mass.

The simulation of the wall-jet is performed by coupling the PDF solver with RPLUS.[3] The Baldwin-Lomax algebraic turbulence model is used in this calculation. The turbulence diffusivity is calculated based on the eddy viscosity and the assumption that the turbulence Schmidt number equals one. The time scale needed in the molecular mixing model of the PDF equation is calculated using $\tau = y^2/\nu_t$, where ν_t is the turbulent viscosity from the algebraic model, and y is the distance from the wall.

The numerical results reported in the present paper are obtained by using a 71×61 grid in the test section. A finer grid had been tested with little change in the solution observed. The PDF solver uses 100 samples per cell and the solution is obtained by averaging over 100 time steps. The CPU time required on a Cray Y-MP is approximately 0.7 ms per time step per cell. The calculation of the chemical reaction accounts for 68% of the total CPU time.

The overview of the solution by the coupled Monte Carlo/finite-volume computation for the wall-jet case is depicted in Figs. 7a–7d showing the contours of temperature and of mass fraction of hydrogen, oxygen, and water vapor, respectively. The peak temperature in this case is approximately 2500 K. The water vapor contour shows that ignition occurs immediately after hydrogen comes in contact with the vitiated air streams. In reality, an ignition delay was observed in the experiment. This failure to predict the ignition point is expected because of the simple chemistry model used. The com-

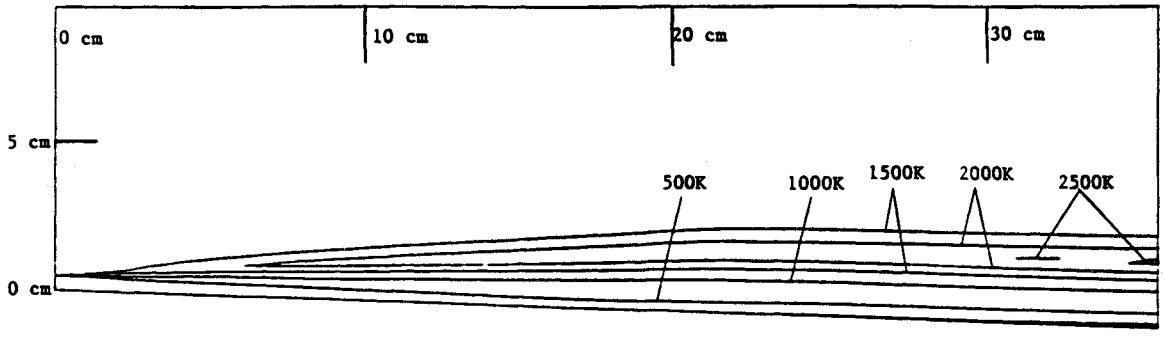

Fig. 7a Temperature contours of PDF solution of the wall-jet case.

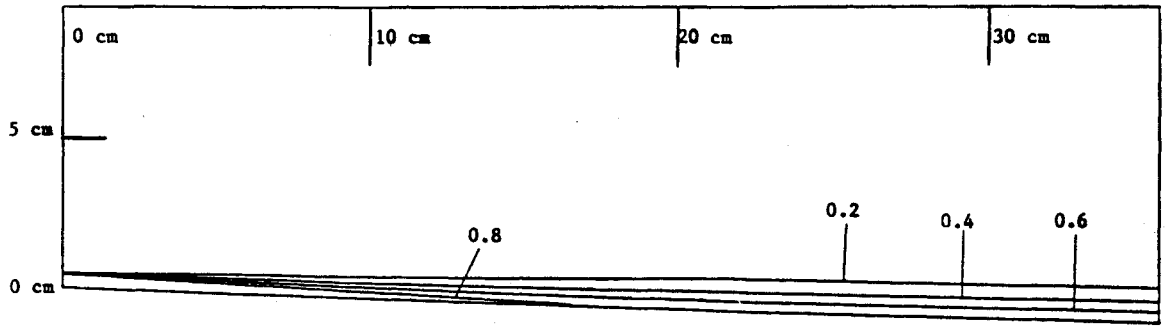

Fig. 7b Hydrogen mass fraction contours of the PDF solution of the wall-jet case.

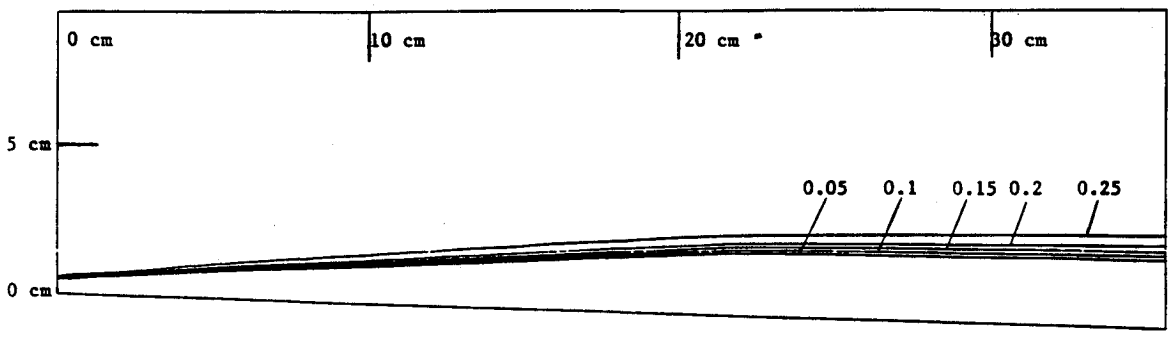

Fig. 7c Oxygen mass fraction contours of the PDF solution of the wall-jet case.

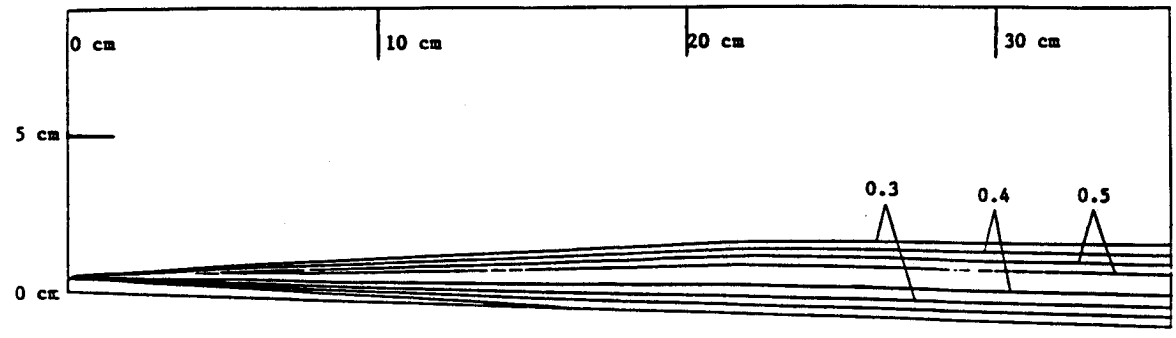

Fig. 7d Water vapor mass fraction contours of the PDF solution of the wall-jet case.

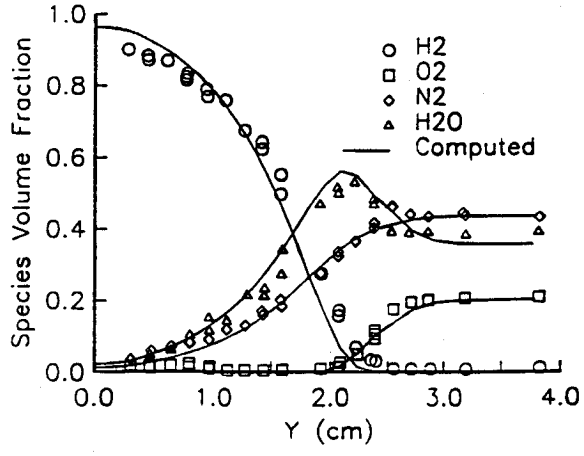

Fig. 8a Composition profiles of the PDF solution for the wall-jet case compared to experimental data (x = 35.6 cm).

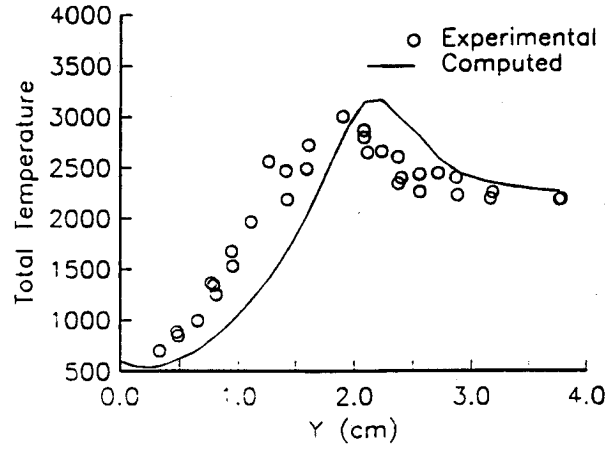

Fig. 8b Total temperature profile of the PDF solution for the wall-jet case compared to experimental data (x = 35.6 cm).

parison of the numerical solution and experimental data measured at the test-section exit is shown in Figs. 8a–8b. The computed species mole fractions shown in Fig. 8a agree very well with the experimental data. The computed total temperature profile, compared to the experimental measurement in Fig. 8b, appears to be shifted away from the wall. However, we believe that the numerical solution for the total temperature is reasonable for the following reason: The profile of water vapor indicates that the distance between the flame surface (peak of water vapor) and the wall is more than 2 cm; because the vitiated air stream has larger total temperature, the peak of total temperature should be farther away from the wall than the flame surface, yet the experimental data seem to indicate otherwise.

In the course of this application, we made the following observations. The accuracy of the Monte Carlo/finite-volume calculation relies on a good estimation of the turbulence diffusivity. For the present test case, the Baldwin-Lomax model seems to be adequate. To understand the effect of the turbulence diffusivity, we experimented with various Schmidt numbers and observed significant changes in species composition. Also noticed was the importance of the lip above the inlet of the hydrogen jet. The lip has a thickness of 0.076 cm. For convenience, we were tempted to ignore this thickness in the computation. However, our experience shows that shrinking the lip thickness to zero can result in a 0.2–0.3-cm shift of the flame surface toward the wall. The presence of any shock wave in the flowfield could also cause the flame surface to shift. As indicated earlier, the chemistry model was responsible for the immediate ignition observed at the lip. The shock wave generated by ignition can reflect from the upper wall and strike the flame, resulting in a shift of the flame surface away from the lower wall. In reality, the ignition point is located a certain distance downstream of the lip, and the reflected shock wave does not interact with the flame in the test section. In our numerical simulation, a nonreflective boundary condition is used at the the upper wall to avoid any shock wave interference.

V. Conclusions

A compressible PDF turbulence model has been developed and implemented in a Monte Carlo solver for two-dimensional elliptic flows. A combined ensemble- and time-averaging scheme is applied, which enables one to use a relatively small sample in the Monte Carlo computation; this averaging scheme greatly improves the efficiency and convergence of the PDF solution, thereby making large-scale computations feasible. The PDF solver can be easily coupled with any existing finite-volume solvers for compressible flows. Numerical results show that, for chemically reacting flows, the PDF method seemed to provide better results than conventional computational fluid dynamics methods.

Acknowledgment

This work is supported by NASA Lewis Research Center under Contract NAS-25266.

References

[1]Pope, S. B., "PDF Methods for Turbulent Reactive Flows," *Progress in Energy Combustion Sciences,* Vol. 11, No. 2, 1985, pp. 119–192.

[2]Pope, S. B., private communication, May, 1992.

[3]Shuen, S., and Yoon, S., "Numerical Study of Chemically Reacting Flows Using a Lower-Upper Symmetric Successive Overrelaxation Scheme," *AIAA Journal,* Vol. 27, No. 12, 1989, pp. 1752–1760.

[4]Raju, M. S., "Heat Transfer and Performance Characteristics of a Dual-Ignition Wankel Engine," Society of Automotive Engineers, SAE paper 920303, Feb. 1992.

[5]Kollmann, W., "The PDF Approach to Turbulent Flow," *Theoretical and Computational Fluid Dynamics,* Vol. 1, No. 5, 1990, pp. 249–285.

[6]Anand, M. S., Pope, S. B., and Mongia, H. C., "Pressure Algorithm for Elliptic Flow Calculations with the PDF Method," *CFD Symposium on Aeropropulsion,* NASA Lewis Research Center, Brook Park, OH, April 24–26, 1990.

[7]Haworth, D. C., and El Tahry, S. H., "Probability Density Function Approach for Multidimensional Turbulent Flow Calculations with Application to in-Cylinder Flows in Reciprocating Engines," *AIAA Journal,* Vol. 29, No. 2, 1991, pp. 208–218.

[8]Roekaerts, D., "Use of a Monte Carlo PDF Method in a Study of the Influence of Turbulent Fluctuations on Selectivity in a Jet-stirred Reactor," *Applied Scientific Research,* Vol. 48, Nos. 3–4, Oct. 1991, pp. 271–300.

[9]Correa, S. M., and Pope, S. B., "Comparison of a Monte Carlo PDF/Finite-Volume Mean Flow Model with Bluff-Body Raman Data," *24th Symposium on Combustion,* The Combustion Inst., Pittsburgh, PA, 1992.

[10]Shih, T.-H., and Lumley, J. L., "A Critical Comparison of Second-Order Closures with Direct Numerical Simulation of Homogeneous Turbulence," NASA TM 105351, Nov. 1991.

[11]Sarkar, S., Erlebacher, G., and Hussaini, M.Y., "Compressible Homogeneous Shear: Simulation and Modeling," NASA CR-189611, 1992.

[12]O'Brien, E. E., "The Probability Density Function Approach to Reacting Turbulent Flows," *Turbulent Reacting Flows,* Springer-Verlag, Berlin, 1980, p. 185.

[13]Pope, S. B., "A Monte Carlo Method for the PDF Equations of Turbulent Reactive Flow," *Combustion Science and Technology,* Vol. 25, No. 5, 1981, p. 159.

[14]Hsu, A. T., and Chen, J. Y., "A Continuous Mixing Model for PDF Simulations and its Applications to Combusting Shear Flows," *Proceedings of the 8th Symposium on Turbulent Shear Flows* (Technical Univ. of Munich, Munich, Germany), Sept. 1991, p. 22-4.

[15]Hsu, A. T., "Study of Hydrogen Diffusion Flames Using Probability Density Function Turbulence Model," AIAA Paper 91-1780, June 1991.

[16]Janicka, J., Kolbe, W., and Kollmann, W., "Closure of the Transport Equation for the Probability Density Function Scalar Field," *Journal of Non-Equilibrium Thermodynamics,* Vol. 4, No. 1, 1979, pp. 47–66.

[17]Villasenor, R., Chen, J.-Y., and Pitz, R. W., "Modeling Ideally Expanded Supersonic Turbulent Jet Flows With Nonpremixed H_2-Air Combustion," *AIAA Journal,* Vol. 30, No. 2, 1992, pp. 395–402.

[18]Rogers, R. C., and Chinitz, W., "Using a Global Hydrogen-Air Combustion Model in Turbulent Reacting Flow Calculations," *AIAA Journal,* Vol. 21, No. 4, 1983, pp. 586–592.

[19]Evans, J. S., Schexnayder, C. J., and Beach, H. L., "Application of a Two-Dimensional Parabolic Computer Program to Prediction of Turbulent Reacting Flows," NASA TP-1169, March 1978.

[20]Eklund, D. R., Drummond, J. P., and Hassan, H. A., "Calculation of Supersonic Turbulent Reacting Coaxial Jets," *AIAA Journal,* Vol. 28, No. 9, 1990, pp. 1633–1641.

[21]Evans, J. S., and Schexnayder, C. J., "Influence of Chemical Kinetics and Unmixedness on Burning in Supersonic Hydrogen Flames," *AIAA Journal,* Vol. 18, No. 2, 1980, pp. 188–193.

[22]Burrows, M. C., and Kurkov, A. P., "Analytical and Experimental Study of Supersonic Combustion of Hydrogen in a Vitiated Air Stream," NASA TM X-2828, 1973.